How to cite: *Angew. Chem. Int. Ed.* **2023,** *62,* e202213980
International Edition: doi.org/10.1002/anie.202213980
German Edition: doi.org/10.1002/ange.202213980

Mechanochemistry

Off-center Mechanophore Activation in Block Copolymers

*Hang Zhang and Charles E. Diesendruck**

Abstract: Block copolymers (BCPs) are used in numerous applications in modern materials science. Yet, like homopolymers, BCPs can undergo covalent bond scission when mechanically stressed (mechanochemistry), which could lead to unexpected consequences in such applications. BCPs' heterogeneity may affect force transduction, perhaps changing force distribution and localization. To verify this, a *gem*-dichlorocyclopropane (*g*DCC) embedded linear chain is prepared and extended with a poly(methyl methacrylate) block. When stressed in solution, the mechanochemical ring-opening of *g*DCC is accelerated compared to homopolymers, even though the mechanophores are at the chain ends. Moreover, a higher mechanophore activation selectivity is obtained. These results indicate that mechanochemical response outside, and even far from the chain center is quite prominent in BCPs, and that forces along the polymer chain can efficiently activate multi-mechanophores regions, even when far from the polymer midchain.

Introduction

Covalent polymer mechanochemistry has been providing new understanding on the relation between mechanical stress and chemical changes in macromolecules, as well as new molecular tools to develop mechanoresponsive functional materials such as stress-reporting,[1] self-healing,[2] drug delivering,[3] and more.[4] With the design, synthesis and incorporation of force-sensitive molecular units, mechanophores,[5] into polymer backbones, one can improve mechanochemical specificity when force is applied and try to achieve mechanoresponse prior to mechanochemical degradation of properties.[6] For instance, *gem*-dihalocyclopropane mechanophores, which undergo mechanically triggered transition to 2,3-dihaloalkenes, have been incorporated into chains as force sensors[7] to investigate mechanochemical selectivity, for example in linear and cyclic polymers.[8] It has also been built upon as a design for the development of mechanoacids.[9]

In parallel to advances in mechanophore design and application, significant efforts have been devoted to understanding the effect of chain architecture and morphology on mechanochemistry rate, relative position, and selectivity.[8b,10] Solution mechanochemistry in star polymers was showed to be governed by the longest molecular spine.[11] More recently, the mechanochemistry in bottlebrushes and dendronized polymers has been reported, in which extremely extended conformations (longer persistence length) enable faster mechanochemistry, and sometimes even in the side-chains.[10a,12] The consistent conformation promoted mechanochemistry was reaffirmed in our recent study in which polymers with higher helicities in the backbone, hence having a longer persistence length, undertook faster mechanochemistry.[13] Conversely, folding the polymer chain with covalent and non-covalent interactions into denser, collapsed conformations with smaller hydrodynamic volumes could significantly slow the mechanochemical crumbling of the backbone, as force focus changes from the main chain center to intramolecular cross-linkers.[14]

Block copolymers (BCPs) have also been a focus of polymer science research, having found numerous applications in nanotechnology, as advanced elastomers, and more.[15] BCPs present a heterogeneous character at the macromolecular chain level resulting from the chemical diversity of constituent blocks, which can lead to microphase separation due to thermodynamic incompatibility.[16] Polymer mechanochemistry should have significant implications in the BCPs' performance, as it occurs during processing and through the polymer life-cycle,[17] and covalent scission would create a population of different copolymers which could disrupt the formation of the intended nanostructures.[18] Moreover, considering the differences in the blocks′ chemistry and morphology, such heterogeneous structures make BCPs promising candidates to study the effect of chain composition on mechanical stress transduction and distribution. Little is known on the covalent mechanochemistry of BCPs, as all examples in the literature describe their mechanochemistry as part of larger micelle structures. Heuts et al. showed that mechanophores can be activated in relatively short polymer chains when these are assembled into micelles.[19] Du and Zhang proposed that a micellar structure made of ABA triblock copolymers comprising a chain-centered spiropyran (SP) mechanophore significantly accelerated the SP mechanochemical electrocyclic ring-opening.[20] More recently, Xu reported self-assembled vesicles which used a diselenide mechanophore

[*] Dr. H. Zhang, Prof. Dr. C. E. Diesendruck
Schulich Faculty of Chemistry, Technion—Israel Institute of Technology
Haifa 3200008 (Israel)
E-mail: charles@technion.ac.il

between the two blocks, which underwent diselenide exchange when under osmotic pressure.[21]

Results and Discussion

To study the mechanochemistry in BCPs, our design includes a block containing multiple *g*DCC mechanophores,[7] called "non-scissile" as their activation is not accompanied by chain scission, to study how a second polyolefin block affects the mechanical transduction towards the mechanophores in BCPs. The BCPs syntheses use a combination of ring opening metathesis polymerization (ROMP) of *gem*-dichlorocyclopropanated cyclooctadiene (*g*DCC-COD) and atom transfer radical polymerization (ATRP) of methyl methacrylate (MMA) in sequential steps (Scheme 1). First, the hydroxide terminated P(*g*DCC) is prepared through the synthesis of sacrificial block copolymers P(*g*DCC-*b*-acetals) by sequential ROMP and subsequent acidolysis of the acetal block.[22] Reaction with 2-bromo-2-methylpropionyl bromide (BIBB) affords macroinitiators P(*g*DCC)–Br, which are used in the ATRP of MMA, affording the different P(*g*DCC-*b*-MMA)s. Representative ^{1}H NMR of hydroxyl-terminated P(*g*DCC)$_{60}$–OH, P(*g*DCC)$_{60}$-Br, and the corresponding BCP of P(*g*DCC$_{60}$-*b*-MMA$_{666}$) are shown in Figure 1a. The proton signal of the terminal CH_2–OH can be seen in the P(*g*DCC)$_{60}$–OH at 4.09 ppm, and shifts downfield to 4.62 ppm when the monotelechelic polymer is functionalized to P(*g*DCC)$_{60}$-Br, indicating the successful and complete coupling between terminal –OH and BIBB. The characteristic signals of MMA (3.53, 0.95, and 0.78 ppm) in the ^{1}H NMR are clearly seen after the ATRP.

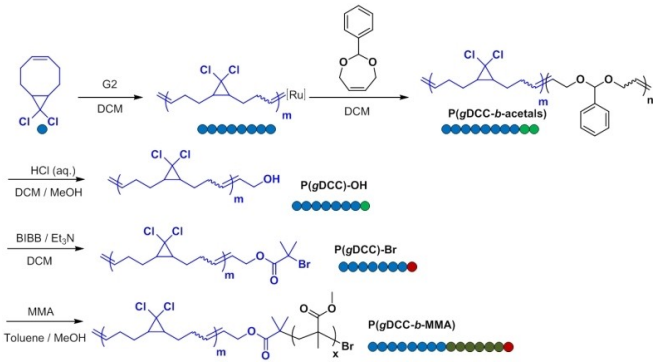

Scheme 1. Synthesis of *g*DCC mechanophore-containing BCPs.

The homopolymers (macroinitiators) and BCPs were additionally characterized by size exclusion chromatography (SEC) with multi-angle light scattering detection (MALS, Figure 1b). The SEC curves show the expected shift to shorter retention times with higher degrees of polymerization (DP), as well as after the copolymerization step. Through numerous preparations of the P(*g*DCC), homopolymers with different lengths were obtained, which could be used either as macroinitiators (Table 1, entries 1–3) or as control homopolymers for comparison (entries 4–5). Given the chain contour length has been shown as a good descriptor to assess the rate of polymer mechanochemistry in linear morphologies,[23] the total numbers of carbon in each backbone (L_c) were calculated from the molecular weight and ^{1}H NMR (in the case of BCPs), and are also listed in Table 1 (an open *g*DCC-COD is <2 % shorter than a MMA tetramer). Three different P(*g*DCC)$_m$-Br macroinitiators ($m=60$, 110, 152) were used to prepare three BCPs. P(*g*DCC$_{60}$-*b*-MMA$_{666}$) and P(*g*DCC$_{152}$-*b*-MMA$_{410}$) have a very similar contour length (L_c around 2000), but very different block composition (8 vs 27 *g*DCC mol %, equivalent to 26 vs 60 *g*DCC length%). P(*g*DCC)$_{256}$ also has a similar L_c but is a homopolymer (100 % *g*DCC) and is therefore used as a control. In addition, P(*g*DCC$_{110}$-*b*-MMA$_{142}$) has a lower L_c of 1164 but higher *g*DCC content (44 mol %, 76 length%), and is used to verify the influence of overall backbone length, especially when compared to homopolymeric P(*g*DCC)$_{167}$, which presents L_c of 1336.

The synthesized polymers (Table 1, entries 1, 4–8) were subjected to pulsed sonication (1 s on, 2 s off, 2 mg mL^{-1} in THF at -10 °C). Aliquots were taken at specific intervals and subsequently analyzed by ^{1}H NMR and SEC-MALS to

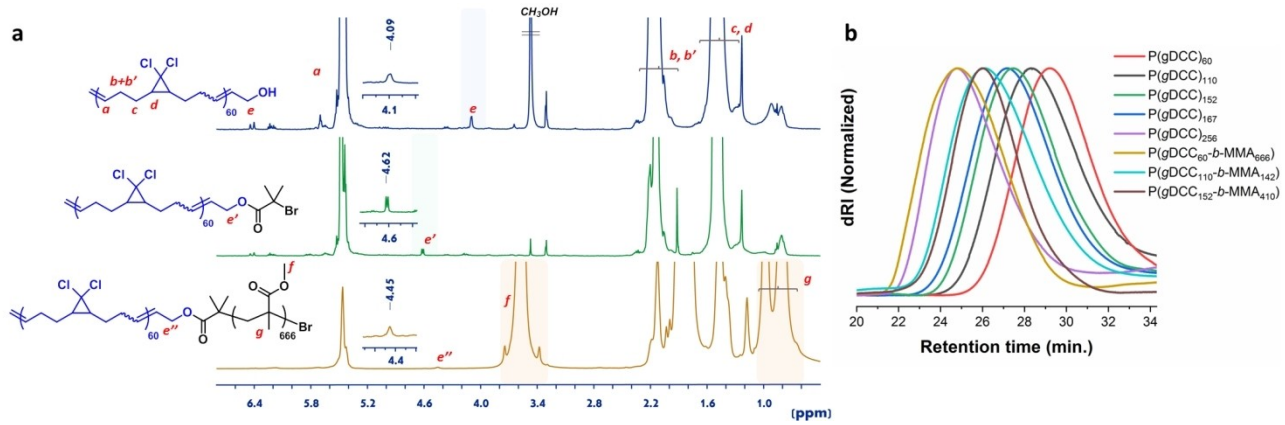

Figure 1. a) Representative ^{1}H NMR spectra (in $CDCl_3$) of P(*g*DCC)$_{60}$–OH, P(*g*DCC)$_{60}$-Br, and P(*g*DCC$_{60}$-*b*-MMA$_{666}$). b) SEC curves (THF, 1 mL min^{-1}, 30 °C, normalized differential refractive index (dRI) signal shown) of P(*g*DCC) and P(*g*DCC-*b*-MMA) used in this study.

Table 1: Characterization of the polymers used in this study.[a]

Entry	Polymers	M_n [kDa][b]	$Đ$[b]	L_c (#atoms)[c] gDCC	MMA	Total	gDCC (mol%)[d]
1	P(*g*DCC)$_{60}$	12	1.16	480	0	480	100
2	P(*g*DCC)$_{110}$	21	1.21	880	0	880	100
3	P(*g*DCC)$_{152}$	29	1.20	1216	0	1216	100
4	P(*g*DCC)$_{167}$	32	1.25	1336	0	1336	100
5	P(*g*DCC)$_{256}$	49	1.29	2048	0	2048	100
6	P(*g*DCC$_{60}$-*b*-MMA$_{666}$)	77	1.36	480	1332	1812	8
7	P(*g*DCC$_{152}$-*b*-MMA$_{410}$)	62	1.18	1216	820	2036	27
8	P(*g*DCC$_{110}$-*b*-MMA$_{142}$)	52	1.23	880	284	1164	44

[a] P(*g*DCC)s were prepared by ROMP, BCPs were obtained by ATRP. [b] Determined by THF SEC-MALS (1 mL min^{-1}, 30 °C). [c] Number of carbon atoms in backbone, $L_c = (DP_{gDCC} \times 8) + (DP_{MMA} \times 2)$. [d] From ^{1}H NMR.

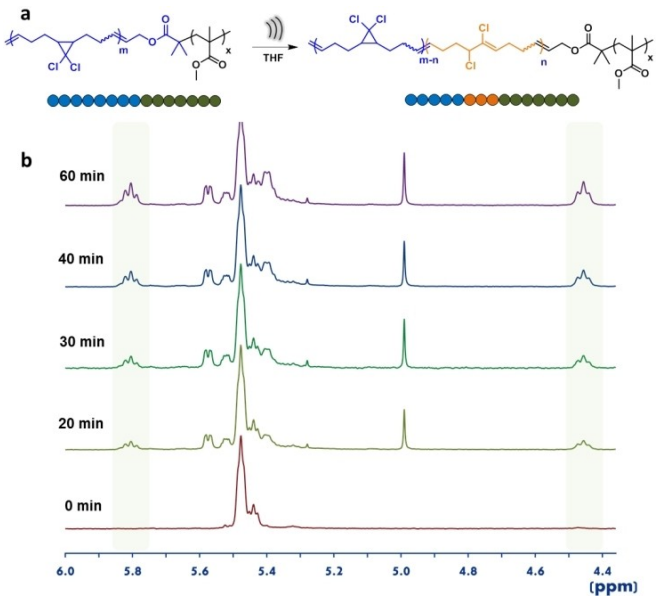

Figure 2. a) Mechanochemical activation of gDCC in a BCP. b) Representative ^{1}H NMR spectra of sonicated P(*g*DCC$_{152}$-*b*-MMA$_{410}$) over sonication time.

assess, respectively, mechanophore activation and non-selective C–C mechanochemistry (chain scission).[8b] In ^{1}H NMR, the signals due to the electrocyclic ring-opening of *g*DCC to 1,2-dichloroalkene at 5.80, 4.46 ppm appear and become stronger with sonication time (Figure 2 and Figures S3–S7). By plotting the activation extent of *g*DCC versus sonication time for different polymers, we see that homopolymer P(*g*DCC)$_{60}$, with the shortest L_c of 480, shows, expectedly, the slowest mechanophore activation (only 5% after 1 h sonication) (Figure 3a). Extending the chain through a PMMA block, provides the BCP made from the short homopolymer, P(*g*DCC$_{60}$-*b*-MMA$_{666}$), with an L_c of 1812. This BCP, on one hand, has a higher L_c making energy transduction from the solution to the chain more efficient; but on the other hand, the *g*DCC are only at the edge of the polymer (26% of the length), a position typically reserved for control experiments for new mechanophores.[6b,24] Surprisingly, this BCP, containing the shortest *g*DCC block amongst the tested polymers, shows faster mechanophore activation than P(*g*DCC$_{152}$-*b*-MMA$_{410}$) and P(*g*DCC)$_{256}$, both of which with very similar L_c but longer *g*DCC blocks (60 vs 100 length%) (Figure 3a). P(*g*DCC$_{60}$-*b*-MMA$_{666}$) and P(*g*DCC)$_{256}$ have, initially, similar retention volumes in the SEC, indicating similar hydrodynamic volume, but significantly different mechanophore activation rates. Meanwhile,

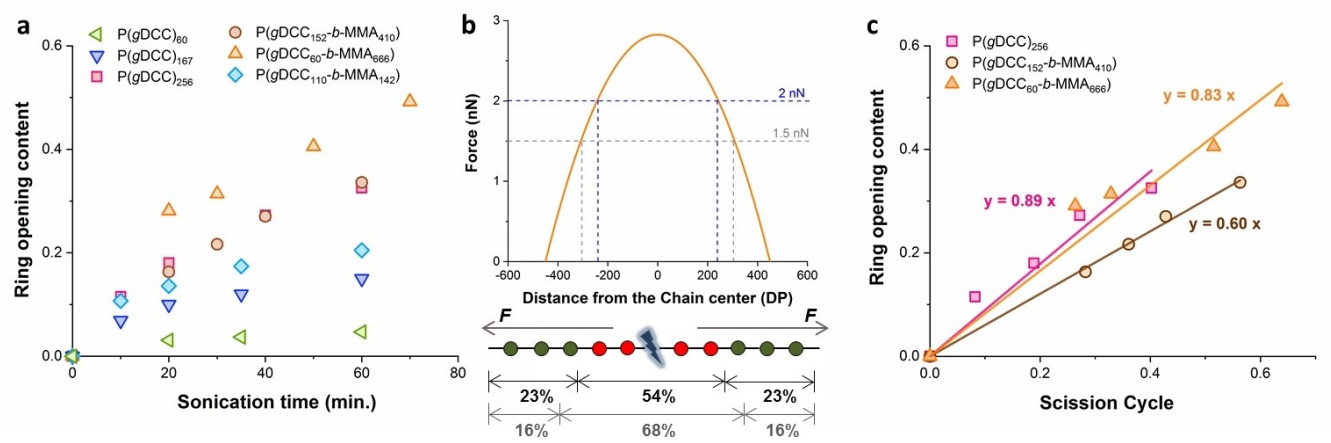

Figure 3. a) Plots of *g*DCC ring-opening content as a function of sonication time for six polymers. b) Modeled theoretical force distribution on a backbone of PMMA$_{900}$. c) *g*DCC ring-opening content as a function of scission cycle for three polymers with ca. 2000 L_c.

P(gDCC$_{152}$-b-MMA$_{410}$) has a smaller hydrodynamic volume, but presents as fast mechanophore activation as P(gDCC)$_{256}$.

Overall, these results indicate that mechanophore activation is accelerated in BCPs, even if the mechanophores are not close to the chain center. Such unexpected faster mechanophore activation in BCPs is further supported by comparing the shorter P(gDCC$_{110}$-b-MMA$_{142}$) with P(gDCC)$_{167}$ (L_c, 1164 vs 1336), in which 21 vs 15 % activation can be seen after 60 min sonication, respectively.

Even though off-center mechanophore activation is typically seen in multi-mechanophore homopolymers (overall activation is typically well above what is in the "center"),[8b] accepted models to simulate the effect of solvodynamic shear on linear macromolecules[25] provide a general expectation that even in multi-mechanophore polymers, activation starts and is faster around the chain center, but can reach the edges if stress values are high enough.[26] This is expected as these models were developed around the numerous experimental support for stress concentration at the chain center.[27] These models do not explain the observations in the experiments described above, as they would lead to faster activation in homopolymers where more mechanophores are exposed to higher forces. As a simple numerical example, following previous studies, we applied the bead-rod model to describe the force experienced by the homopolymers' chain segments on the microsecond timescale.[8b,26a] The force distribution along the chain of a homopolymer PMMA$_{900}$ having a similar L_c to P(gDCC$_{60}$-b-MMA$_{666}$) shows a typical parabolic distribution peaking at the chain center (Figure 3b). Following previous uses of this model to study gDCC activation, a force of 2 nN was set as the limit to trigger the ring opening of gDCC,[28] which would cover 54 % of the central segments of the chain, leaving 23 length% in the BCP edge outside the region where force is enough to activate the gDCC. Given the length portion of gDCC in this BCP is 26 %, only 3/26 (11.5 % of the mechanophore) would be mechanically activated, and at a slower rate. The 2 nN force used for estimation of ring opening of gDCC was calculated from the 1.3 nN measured by force spectroscopy studies on gDCC-functionalized poly(butadiene), through extrapolation to the time scale of ultrasonication (10^{-6} s).[28] If one considers the numerous plausible errors in this model: 20 % error in the cantilever calibration, and a reduction in triggering force to 1.5 nN, the activation value is increased to 38 %, which is still lower than the experimental observation in P(gDCC$_{60}$-b-MMA$_{666}$). However, if we double the strain rate in sonication,[29] then not only forces capable of C–C activation are seen, but gDCC activation reaches 73 %, beyond what was seen in the experiment. Still, in P(gDCC$_{60}$-b-MMA$_{666}$) BCP, the gDCC in this edge area is not only activated, it does so faster than in the control homopolymer (Figure S9). Clearly, this model, which has its own limitations, is noticeably not representing experimental observations in BCPs. Given the BCPs used here are made of chemically compatible blocks, in a good solvent for both blocks, these chains are expected to assume a random coil conformation, similar to a homopolymer. The absence of aggregates or assemblies of such BCPs in THF was confirmed by dynamic light scattering measurements (Figure S10), indicating the divergence in gDCC activation kinetics in BCPs only results from the differential polymer structure. In linear homopolymers, it is accepted that stress concentrates at the chain center, leading to backbone scission (i.e., C–C activation) or mechanophore activation, and there is ample evidence to support this.[8b,25,30] In the development of numerous mechanophores, installing it at the chain edge has been used as a control experiment, to compare thermal vs. mechanical activation, as it "cannot" be activated mechanically.[1b,31] Still, linear BCP chains tested here show a result that cannot be predicted by this assumption and therefore, a new model needs to be developed to understand stress distribution in linear architectures that would also explain the mechanophore activation at the edges of BCPs.

To provide additional insights into the mechanical degradation of the BCPs which could affect their performance, SEC-MALS analysis was used to measure the rate of C–C bond scission, which can then be compared to mechanophore activation.[14a] As expected, the SEC peaks of the polymers are continuously shifting towards longer retention times with longer sonication periods, indicating that in addition to mechanophore activation, chain scission events are occurring (see Figures S11–S13). Given gDCC activation does not affect M_n, the changes in molecular weight can be used to calculate the number of average C–C bond scissions as a function of sonication time. We thus found that even having similar contour length, the two BCPs, P(gDCC$_{60}$-b-MMA$_{666}$) and P(gDCC$_{152}$-b-MMA$_{410}$) underwent remarkably different extents of C–C bond scissions compared to homopolymeric P(gDCC)$_{256}$. As seen in Figure S14, both BCPs exhibit a faster backbone scission compared to P(gDCC)$_{256}$. Such difference is expected as gDCC activation dissipates mechanical energy and therefore alleviate stress in the backbone, inhibiting C–C bond scission.[7] Still, this is probably not the only factor as the two BCPs show similar C–C scission rate despite their different lengths of gDCC blocks.

With data on both mechanophore activation and backbone scission, the mechanophore activation selectivity can be studied using the extent of ring-opening extrapolated to one scission cycle (ϕ), as defined by Craig,[8b] which can be obtained from plots of gDCC ring-opening versus chain scission cycle, where ϕ is the slope of the associated linear fit (Figure 3c). ϕ values of 0.89, 0.83, and 0.60 were obtained for the three polymers with similar L_c: P(gDCC)$_{256}$, P(gDCC$_{60}$-b-MMA$_{666}$), and P(gDCC$_{152}$-b-MMA$_{410}$), respectively. The selectivity value for P(gDCC)$_{256}$ is consistent with that reported by Craig et al., who measured a 0.92 for P(gDCC)$_{306}$ (slightly larger length).[8b] P(gDCC$_{60}$-b-MMA$_{666}$) unexpectedly presents a similar selectivity. The BCP, with similar contour length, has all its gDCC far from the chain center. This is probably a combination of two factors, as described above, on one hand, gDCC is more rapidly activated, dissipating mechanical energy, and on the other hand, C–C bond scission is accelerated, even with similar L_c. Overall, all the mechanochemical reactions are accelerated in the BCP. In P(gDCC$_{152}$-b-MMA$_{410}$) these two effects do not balance out, as gDCC is not significantly accelerated (it

is quite similar to the homopolymer), but C–C bond scission is faster, leading to lower selectivity. This polymer shows similar mechanophore activation rate to P(*g*DCC)$_{256}$, but faster non-selective mechanochemistry, again, indicating that mechanochemistry is accelerated in BCPs.

Conclusion

To summarize, this study presents, for the first time, the morphological effect of having two different blocks on the polymer mechanochemistry of linear chains in solution. Through the use of non-scissile multiple mechanophores P(*g*DCC) to build the macro-initiator, several block copolymers were prepared with similar lengths to the respective control homopolymers. Measuring the *g*DCC activation kinetics and the related selectivity between activation and non-selective C–C bond scission in these BCPs unveiled an unusual shear force transduction and distribution along BCP chains compared to P(*g*DCC) homopolymers, with significant and faster *g*DCC activation at the edges of BCP chains, as well as accelerated non-selective C–C bond scission. While an overall polymer length is still required to gather enough energy from environment created by the solvodynamic shear, it seems like the presence of two blocks leads to changes compared to the parent's homopolymer chain creating increased stress concentration off chain-center, accelerating mechanophore activation at the polymer edges. The bead-rod model was applied but it is based on a concept that stress is higher at the chain center, and therefore fails to explain the higher mechanochemistry kinetics in BCPs, indicating that new models are required to describe solution polymer mechanochemistry in BCPs. These results provide initial information on the risks of block-copolymer mechanochemistry, which could lead to the loss of their unique characteristics; but also provide the promise of mechanochemistry and mechanophore activation at positions which are very far from the chain center, creating new possibilities in designing mechanoresponsive functional materials based on the (self-)assembly of block copolymers.

Acknowledgements

The authors acknowledge the Israel Science Foundation (Grant No. 354/19) for financial support.

Conflict of Interest

The authors declare no conflict of interest.

Data Availability Statement

The data that support the findings of this study are available in the Supporting Information of this article.

Keywords: Block Copolymers · Force-Distribution · Mechanochemistry · Stress-Response

[1] a) Y. Chen, A. J. H. Spiering, S. Karthikeyan, G. W. M. Peters, E. W. Meijer, R. P. Sijbesma, *Nat. Chem.* **2012**, *4*, 559–562; b) D. A. Davis, A. Hamilton, J. Yang, L. D. Cremar, D. Van Gough, S. L. Potisek, M. T. Ong, P. V. Braun, T. J. Martinez, S. R. White, J. S. Moore, N. R. Sottos, *Nature* **2009**, *459*, 68–72; c) K. Imato, A. Irie, T. Kosuge, T. Ohishi, M. Nishihara, A. Takahara, H. Otsuka, *Angew. Chem. Int. Ed.* **2015**, *54*, 6168–6172; *Angew. Chem.* **2015**, *127*, 6266–6270.

[2] a) C. E. Diesendruck, N. R. Sottos, J. S. Moore, S. R. White, *Angew. Chem. Int. Ed.* **2015**, *54*, 10428–10447; *Angew. Chem.* **2015**, *127*, 10572–10593; b) Z. S. Kean, S. L. Craig, *Polymer* **2012**, *53*, 1035–1048.

[3] a) S. Huo, P. Zhao, Z. Shi, M. Zou, X. Yang, E. Warszawik, M. Loznik, R. Gostl, A. Herrmann, *Nat. Chem.* **2021**, *13*, 131–139; b) R. Kung, R. Gostl, B. M. Schmidt, *Chem. Eur. J.* **2022**, *28*, e202103860.

[4] a) Z. Chen, X. Zhu, J. Yang, J. A. M. Mercer, N. Z. Burns, T. J. Martinez, Y. Xia, *Nat. Chem.* **2020**, *12*, 302–309; b) Y. Zhang, Z. Wang, T. B. Kouznetsova, Y. Sha, E. Xu, L. Shannahan, M. Fermen-Coker, Y. Lin, C. Tang, S. L. Craig, *Nat. Chem.* **2021**, *13*, 56–62; c) J. Li, C. Nagamani, J. S. Moore, *Acc. Chem. Res.* **2015**, *48*, 2181–2190.

[5] a) G. De Bo, *Macromolecules* **2020**, *53*, 7615–7617; b) Y. Chen, G. Mellot, D. van Luijk, C. Creton, R. P. Sijbesma, *Chem. Soc. Rev.* **2021**, *50*, 4100–4140.

[6] a) H. Qian, N. S. Purwanto, D. G. Ivanoff, A. J. Halmes, N. R. Sottos, J. S. Moore, *Chem* **2021**, *7*, 1080–1091; b) M. M. Caruso, D. A. Davis, Q. Shen, S. A. Odom, N. R. Sottos, S. R. White, J. S. Moore, *Chem. Rev.* **2009**, *109*, 5755–5798; c) M. B. Larsen, A. J. Boydston, *J. Am. Chem. Soc.* **2013**, *135*, 8189–8192; d) G. R. Gossweiler, G. B. Hewage, G. Soriano, Q. Wang, G. W. Welshofer, X. Zhao, S. L. Craig, *ACS Macro Lett.* **2014**, *3*, 216–219.

[7] J. M. Lenhardt, A. L. Black, S. L. Craig, *J. Am. Chem. Soc.* **2009**, *131*, 10818–10819.

[8] a) Y. Lin, Y. Zhang, Z. Wang, S. L. Craig, *J. Am. Chem. Soc.* **2019**, *141*, 10943–10947; b) J. M. Lenhardt, A. L. Black Ramirez, B. Lee, T. B. Kouznetsova, S. L. Craig, *Macromolecules* **2015**, *48*, 6396–6403.

[9] a) Y. Lin, T. B. Kouznetsova, S. L. Craig, *J. Am. Chem. Soc.* **2020**, *142*, 99–103; b) C. E. Diesendruck, B. D. Steinberg, N. Sugai, M. N. Silberstein, N. R. Sottos, S. R. White, P. V. Braun, J. S. Moore, *J. Am. Chem. Soc.* **2012**, *134*, 12446–12449.

[10] a) G. I. Peterson, J. Noh, M. Y. Ha, S. Yang, W. B. Lee, T.-L. Choi, *Macromolecules* **2021**, *54*, 4219–4226; b) A. Levy, H. Goldstein, D. Brenman, C. E. Diesendruck, *J. Polym. Sci.* **2020**, *58*, 692–703; c) F. Wang, M. Burck, C. E. Diesendruck, *ACS Macro Lett.* **2017**, *6*, 42–45; d) A. C. Overholts, M. E. McFadden, M. J. Robb, *Macromolecules* **2022**, *55*, 276–283.

[11] D. C. Church, G. I. Peterson, A. J. Boydston, *ACS Macro Lett.* **2014**, *3*, 648–651.

[12] a) G. I. Peterson, K. T. Bang, T. L. Choi, *J. Am. Chem. Soc.* **2018**, *140*, 8599–8608; b) J. Noh, G. I. Peterson, T.-L. Choi, *Angew. Chem. Int. Ed.* **2021**, *60*, 18651–18659; *Angew. Chem.* **2021**, *133*, 18799–18807.

[13] H. Zhang, C. E. Diesendruck, *Angew. Chem. Int. Ed.* **2022**, *61*, e202115325; *Angew. Chem.* **2022**, *134*, e202115325.

[14] a) A. Levy, F. Wang, A. Lang, O. Galant, C. E. Diesendruck, *Angew. Chem. Int. Ed.* **2017**, *56*, 6431–6434; *Angew. Chem.* **2017**, *129*, 6531–6534; b) A. Levy, R. Feinstein, C. E. Diesendruck, *J. Am. Chem. Soc.* **2019**, *141*, 7256–7260; c) A. Levy, E. Gaver, F. Wang, O. Galant, C. E. Diesendruck, *Chem. Commun.* **2017**, *53*, 10132–10135.

[15] a) A.-V. Ruzette, L. Leibler, *Nat. Mater.* **2005**, *4*, 19–31; b) C. Li, Q. Li, Y. V. Kaneti, D. Hou, Y. Yamauchi, Y. Mai, *Chem. Soc. Rev.* **2020**, *49*, 4681–4736; c) J. Min, D. Barpuzary, H. Ham, G.-C. Kang, M. J. Park, *Acc. Chem. Res.* **2021**, *54*, 4024–4035.
[16] F. S. Bates, G. H. Fredrickson, *Annu. Rev. Phys. Chem.* **1990**, *41*, 525–557.
[17] a) N. Willis-Fox, E. Rognin, T. A. Aljohani, R. Daly, *Chem* **2018**, *4*, 2499–2537; b) J. F. Patrick, M. J. Robb, N. R. Sottos, J. S. Moore, S. R. White, *Nature* **2016**, *540*, 363–370.
[18] C. Choi, S. Ahn, J. K. Kim, *Macromolecules* **2020**, *53*, 4577–4580.
[19] H. Li, R. Göstl, M. Delgove, J. Sweeck, Q. Zhang, R. P. Sijbesma, J. P. A. Heuts, *ACS Macro Lett.* **2016**, *5*, 995–998.
[20] L.-J. Wang, X.-J. Zhou, X.-H. Zhang, B.-Y. Du, *Macromolecules* **2016**, *49*, 98–104.
[21] J. Xia, P. Zhao, S. Pan, H. Xu, *ACS Macro Lett.* **2019**, *8*, 629–633.
[22] S. Hilf, E. Berger-Nicoletti, R. H. Grubbs, A. F. Kilbinger, *Angew. Chem. Int. Ed.* **2006**, *45*, 8045–8048; *Angew. Chem.* **2006**, *118*, 8214–8217.
[23] a) P. A. May, N. F. Munaretto, M. B. Hamoy, M. J. Robb, J. S. Moore, *ACS Macro Lett.* **2016**, *5*, 177–180; b) M. Schaefer, B. Icli, C. Weder, M. Lattuada, A. F. M. Kilbinger, Y. C. Simon, *Macromolecules* **2016**, *49*, 1630–1636.
[24] C. E. Diesendruck, L. Zhu, J. S. Moore, *Chem. Commun.* **2014**, *50*, 13235–13238.
[25] H. Zhang, Y. Lin, Y. Xu, W. Weng in *Polymer Mechanochemistry, Vol. 369* (Eds.: R. Boulatov), Springer International Publishing, Chem, **2015**, pp. 135–207.
[26] a) A. C. Overholts, M. J. Robb, *ACS Macro Lett.* **2022**, *11*, 733–738; b) P. A. R. Glynn, B. M. E. Van Der Hoff, P. M. Reilly, *J. Macromol. Sci. A* **1972**, *6*, 1653–1664.
[27] a) K. L. Berkowski, S. L. Potisek, C. R. Hickenboth, J. S. Moore, *Macromolecules* **2005**, *38*, 8975–8978; b) K. S. Suslick, *MRS Bull.* **1995**, *20*, 29–34; c) B. M. E. Van Der Hoff, P. A. R. Glynn, *J. Macromol. Sci. A* **1974**, *8*, 429–449.
[28] a) H. M. Klukovich, T. B. Kouznetsova, Z. S. Kean, J. M. Lenhardt, S. L. Craig, *Nat. Chem.* **2013**, *5*, 110–114; b) B. Lee, Z. Niu, J. Wang, C. Slebodnick, S. L. Craig, *J. Am. Chem. Soc.* **2015**, *137*, 10826–10832.
[29] M. W. A. Kuijpers, P. D. Iedema, M. F. Kemmere, J. T. F. Keurentjes, *Polymer* **2004**, *45*, 6461–6467.
[30] P. A. May, J. S. Moore, *Chem. Soc. Rev.* **2013**, *42*, 7497–7506.
[31] Q. Qi, G. Sekhon, R. Chandradat, N. M. Ofodum, T. Shen, J. Scrimgeour, M. Joy, M. Wriedt, M. Jayathirtha, C. C. Darie, D. A. Shipp, X. Liu, X. Lu, *J. Am. Chem. Soc.* **2021**, *143*, 17337–17343.

Manuscript received: September 21, 2022
Accepted manuscript online: November 17, 2022
Version of record online: December 7, 2022